

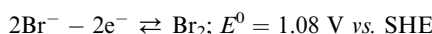
Cite this: *Chem. Sci.*, 2021, **12**, 10878

All publication charges for this article have been paid for by the Royal Society of Chemistry

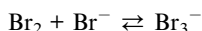
Received 3rd May 2021
Accepted 13th July 2021

DOI: 10.1039/d1sc02434e
rsc.li/chemical-science

The bromine–bromide redox couple plays an essential role in diverse energy storage devices including hydrogen–bromine, zinc–bromine, quinone–bromine, vanadium–bromide and bromide–polysulphide flow batteries.^{1–5} The Br_2/Br^- redox couple is attractive as a cathode reaction due to its high standard potential, large solubility of both reagents, high power density and cost efficiency.⁶ The performance of such devices is generically limited by the thermodynamics and kinetics of the redox couple comprising the battery with fast ('reversible') electron transfer is essential. In many cases, including the Br_2/Br^- couple the electrode reaction involves more than one electron as given in the stoichiometric reaction:



with, at high bromide concentrations, the possibility of the follow up chemical reaction⁷



Since electrons are usually transferred sequentially this implies that the mechanism is multistep with any of the individual mechanistic steps in principle being rate limiting. For this reason catalysts are commonly required to enhance the electrode kinetics at otherwise favourable electrode materials. One type of catalyst which has seen wide usage, including for the Br_2/Br^- couple^{8,9} are carbon nanotubes (CNTs) with suggested advantages which include high surface area and the inherent porosity of CNT composites.¹⁰ The deployment of CNTs as a porous composite presents a further level of

complexity to the electrode reaction beyond its multistep character because of the ill-defined mass transport within the porous layer. In particular ascertaining the intrinsic electron transfer kinetics and hence the level of catalysis, if any, is essentially impossible since these are masked in the voltammetric response by diffusional mass transport effects.^{11–14} Specifically the transport within the porous structure of CNT layers is dominated by thin-layer and other^{15,16} effects which give the illusion of electrochemical reversibility. In order to unscramble possible electro-catalysis of the bromine/bromide couple a different approach is needed.

In the following we study both the electro-oxidation of bromide (BOR) and the electro-reduction of bromine (BRR) at *single* MWCNTs *via* 'nano-impact (aka 'single entity') electrochemistry'^{17–20} in aqueous solution. In this approach a micro-wire electrode at a fixed potential is inserted in a suspension of CNTs in the solution of interest. From time to time a single CNT impacts the electrode, adopts the potential of the latter for the duration of the impact which in the case of CNTs can vary from 1–100 of seconds^{21–23} and sustained catalytic currents flow if the oxidation/reduction of interest is faster at the nanotube in comparison with the micro-wire electrode. The catalytic currents are studied as a function of potential revealing the electron transfer kinetics. Fig. 1 shows the concept of the experiment.

The BOR and BRR were studied first, however, voltammetrically at an unmodified glassy carbon (GC) electrode as shown in Fig. 2 (black line) using 5.0 mM solutions of either NaBr or Br_2 in 0.1 M HNO_3 . The midpoint potential was 0.82 V *versus* the saturated calomel electrode (SCE) consistent with the literature values for the formal potential of the Br_2/Br^- couple.²⁴ The voltammograms were analysed to give transfer coefficients of 0.45 ± 0.01 and 0.33 ± 0.01 (ESI, Section 2†) for the BOR and BRR respectively. Both processes were inferred to be diffusional and the diffusion coefficients D_{Br^-} and D_{Br_2} were calculated to be $2.05 (\pm 0.04) \times 10^{-5} \text{ cm}^2 \text{ s}^{-1}$ and $1.50 (\pm 0.04) \times 10^{-5} \text{ cm}^2 \text{ s}^{-1}$

Department of Chemistry, Physical and Theoretical Chemistry Laboratory, Oxford University, South Parks Road, Oxford OX1 3QZ, UK. E-mail: richard.compton@chem.ox.ac.uk

† Electronic supplementary information (ESI) available. See DOI: 10.1039/d1sc02434e



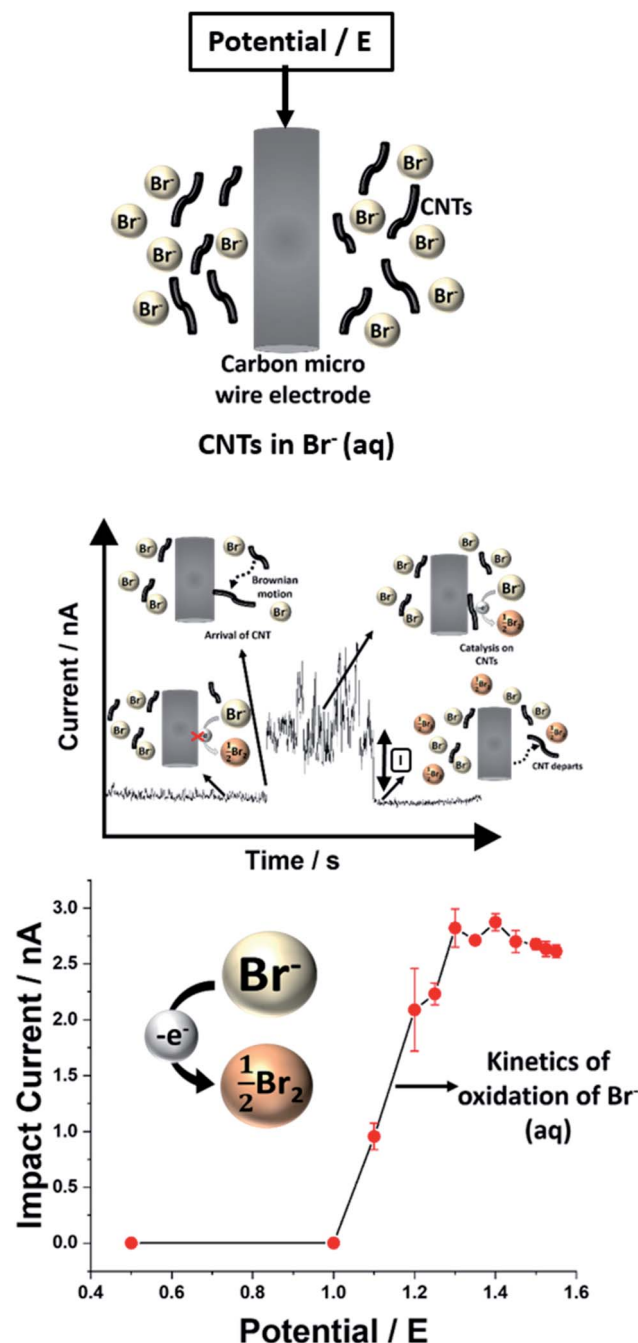


Fig. 1 Schematic representation of 'nano-impact' electrochemistry on a carbon micro wire electrode for the oxidation of aqueous bromide from which the kinetics of the BOR are inferred. Analogous experiments but showing negative impact currents allow the inference of the kinetics of the BRR.

(ESI, Section 3†) using the Randles-Ševčík equation for an irreversible reaction the values are consistent with literature reports.²⁴ Then the electrodes were modified with 30 μg of MWCNTs consisting of *ca.* 125 monolayers (the calculation is given in the ESI, Section 9†) of MWCNTs assuming that they are closely packed across the area of the GC electrode, and the resulting voltammograms are shown in Fig. 2 (red line). In comparison with the unmodified electrode, enhanced currents

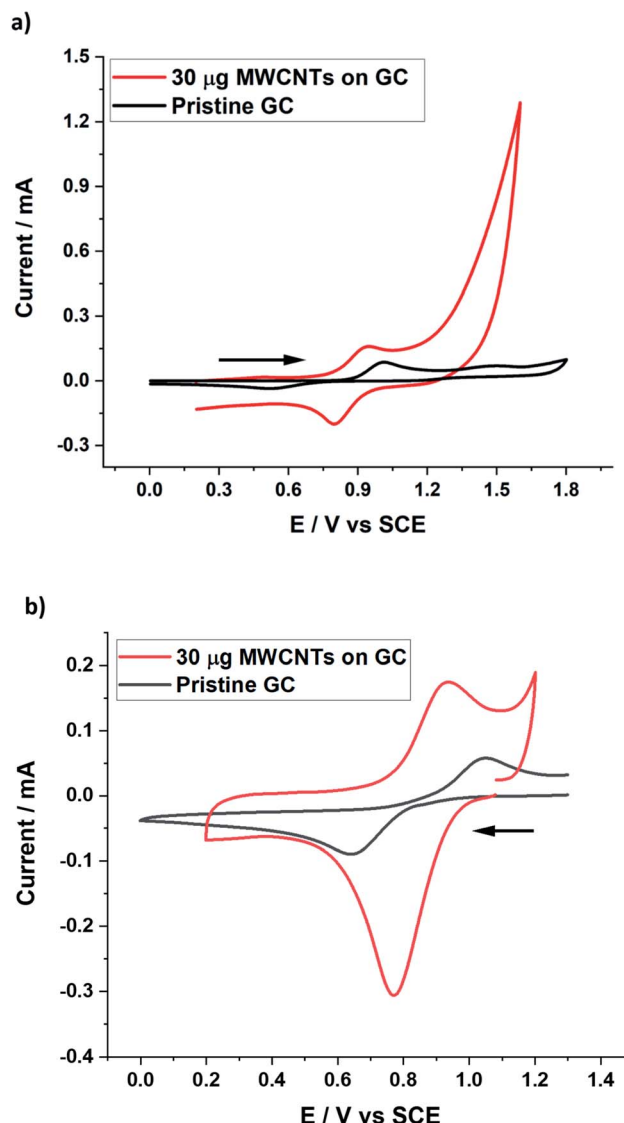


Fig. 2 Cyclic voltammograms at pristine GC (black line) and 30 μg MWCNTs dropcast on GC (red line) at a scan rate of 0.05 V s^{-1} (a) for the bromide oxidation reaction (BOR) in 5.0 mM NaBr in 0.1 M HNO_3 , (b) for the bromine reduction reaction (BRR) in 5.0 mM bromine in 0.1 M HNO_3 .

are seen for the Br_2/Br^- couple which partly reflects the enhanced capacitance of the interface reflecting in turn the large surface area of the deposited nanotubes (*ca.* 60–120 cm^2). Larger signals are also seen indicating a thin layer contribution from the material occluded within the porous layer which also leads to the *apparently* quasi-reversible shape of the voltammograms obtained for both reactions. A log-log plot of peak current (I_p) vs. scan rate (v) showed a gradient value of 0.68 (± 0.01) and 0.66 (± 0.03) for the BOR and BRR (ESI, Section 4†) confirming a mixed mass transport regime^{12,14} with a combination of semi-infinite diffusion and thin layer behaviour. The transition from the fully irreversible to the *apparently* quasi-reversible character is sometimes confused with electrocatalysis attributed to the CNTs rather than thin-layer diffusion. In order to ascertain the true catalytic response, single

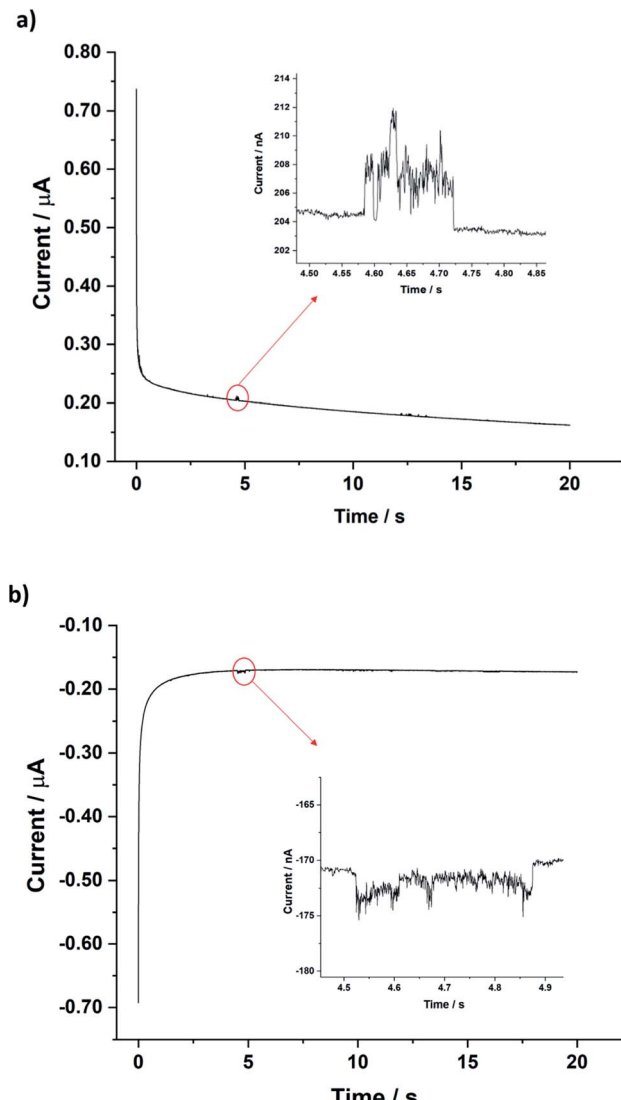


Fig. 3 Chronoamperograms showing the impact step current (a) for the BOR in 5.0 mM NaBr in 0.1 M HNO_3 at 1.3 V vs. SCE, (b) for the BRR in 5.0 mM bromine in 0.1 M HNO_3 at 0.2 V vs. SCE.

entity electrochemistry was measured to obtain the BOR and BRR responses at single CNTs.

For single entity measurements, a clean carbon wire (CWE, length 1 mm and diameter 7 μm) working electrode was used. Chronoamperograms were recorded at a constant applied potential of 0.2 V vs. SCE and 1.3 V vs. SCE for the BOR and BRR respectively (5.0 mM solutions). These values were selected in the light of Fig. 2 to provide a large overpotential for each reaction. Clear oxidative and reductive current steps were observed (Fig. 3). These were ascribed to the arrival of a MWCNT at the electrode surface and the resulting catalytic electron transfer for the duration of the impact. No steps were observed in the absence of MWCNTs (ESI, Fig. S4†). The average residence time of the MWCNT was 1.2 (± 0.5) seconds and the frequency of the collisions was 0.3 (± 0.1) impacts per second. The average impact current for the BOR at 1.3 V vs. SCE was 2.8 (± 0.2) nA (65 impacts) and for the BRR at 0.2 V vs. SCE it was 3.8 (± 0.1) nA (70 impacts). The impact currents were

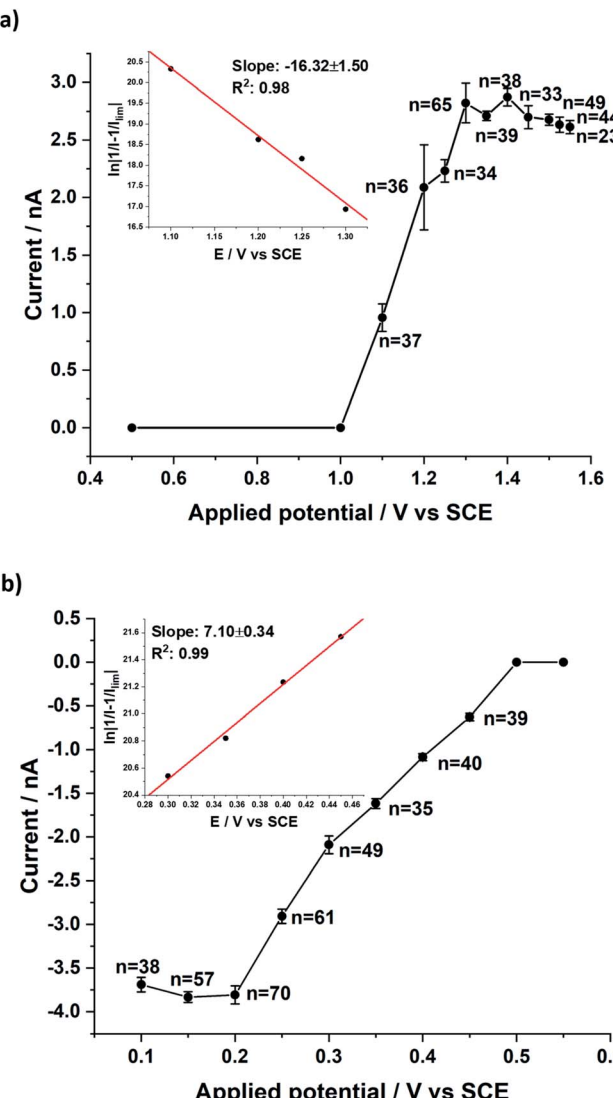


Fig. 4 Average step currents observed as a function of applied potential (a) for the BOR in 5.0 mM NaBr in 0.1 M HNO_3 at, (b) for the BRR in 5.0 mM bromine in 0.1 M HNO_3 ; insets in both the cases show mass transport corrected Tafel analyses.

assumed to be entirely faradaic since control experiments in 0.1 M HNO_3 solution in the presence of 100 μg of MWCNTs (in the absence of Br^- and Br_2) showed no obvious impacts as shown in ESI Section 10.†

Further, impacts for both the BOR and BRR were observed at various potentials (ESI, Section 11†) and analysed to obtain the average faradaic current at each potential. The average impact step current was plotted against the applied potential (Fig. 4). Two sigmoidal curves were obtained reflecting the current-potential response for either the bromide oxidation (BOR) or the bromine reduction (BRR). The curves reflect the average voltammograms (current-potential characteristics) for the Br_2/Br^- redox reaction at *single* carbon nanotubes. The shape of the two sigmoidal curves reflects the onset of electrolysis followed by a diffusion controlled plateau at high over-potentials.²⁵ Mass transport corrected Tafel analysis (Fig. 4; inset) showed the transfer coefficients β to be *ca.* 0.42 and α to be *ca.* 0.20 from the

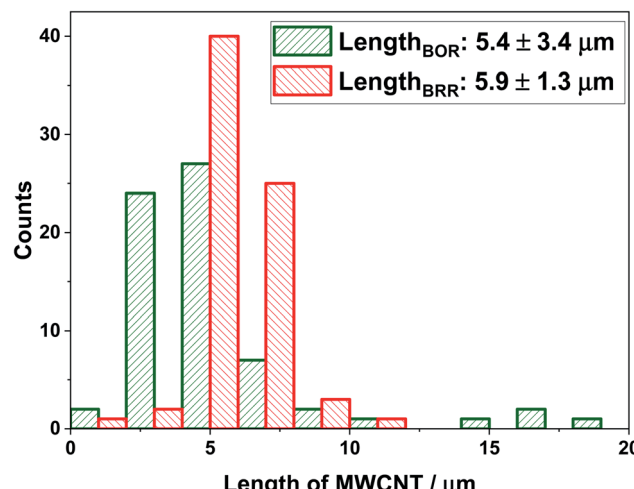
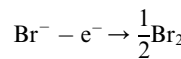


Fig. 5 The length of MWCNTs calculated from the impact currents for the BOR (at 1.3 V vs. SCE) and BRR (at 0.2 V vs. SCE).

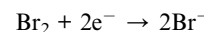
impacts for the BOR and BRR respectively (ESI, Section 6†). The length distribution of the MWCNTs was calculated (ESI, Section 6†) from the currents recorded at potentials corresponding to the plateau in Fig. 4 assuming that the reactions are (Fickian) diffusion controlled at the potentials used and by modelling the CNTs as cylindrical electrodes²¹ assuming a nanotube radius of 15 (± 5) nm and the diffusion coefficients reported above. Chronoamperometry was also conducted for the BOR and BRR in the absence of MWCNTs at 1.3 V and 0.2 V vs. SCE respectively to confirm that no impact currents were contributed by the redox species in the electrolyte (ESI, Section 5†). Alongside, chronoamperograms in 0.1 M HNO₃ and 100 μ g show that the impact current was contributed only by the Br[−] and Br₂ redox reaction and the results are shown in the ESI, Section 10.†

The lengths were found to be 5.4 (± 3.4) μ m (BOR) and 5.9 (± 1.3) μ m (BRR) and are given in Fig. 5 (see ESI, Section 7† for calculations). These values were compared with previously reported dark-field optical microscopy data and good agreement was observed with the literature value of 5.3 (± 2.1) μ m.²⁶ The observed consistency provides strong support for the choice of modelling the single entity voltammetry by analogy with that of a cylindrical electrode.

It is evident that the single entity measurements allow a clear analysis of the catalytic behaviour of the carbon nanotubes by providing a well-defined diffusional regime conducive to the extraction of the electrode kinetics of both the bromide oxidation and the bromine reduction process. In contrast, electrodes were formed by ensembles of carbon nanotubes in the form of a porous layer where the mixed transport regime is not amenable to ready modelling and the dissection of thin-layer effects from the measured voltammetry. The electron transfer kinetics for both the BOR and BRR at single MWCNTs was then obtained *via* full simulation of the two single entity 'voltammograms' using the above measured diffusion coefficients and again treating the impacted MWCNT as a cylindrical electrode with uniform diffusional access and further assuming Butler–Volmer kinetics. For the BOR, one electron transfer was considered as given below,



For the BRR the two electron transfer was modelled as,



The set of parameters used for the analysis are given in the ESI, Section 8.† By using the transfer coefficients deduced from Fig. 4, the only unknown is the standard electrochemical rate constant k which is determined by fitting the impact voltammogram measured relative to a formal potential for the Br₂/Br[−] couple of 0.82 V vs. SCE obtained from the voltammogram at pristine GC. Fig. 6 shows the fitting for the BOR and the BRR with rate constants k_{BOR} of $1.0 (\pm 0.1) \times 10^{-3}$ cm s^{−1} and k_{BRR} of $5.0 (\pm 0.1) \times$

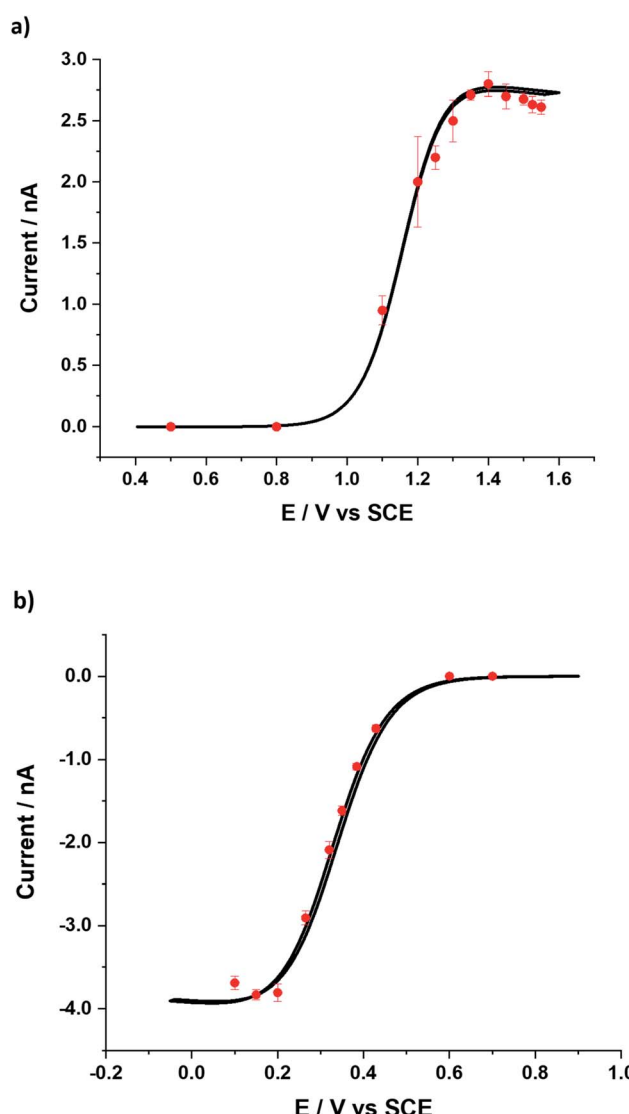


Fig. 6 DIGISIM simulated curves (black line) for average impact currents obtained at different potentials (red circles) (a) for the BOR with a rate constant (k_{BOR}) of $1.0 (\pm 0.1) \times 10^{-3}$ cm s^{−1}, (b) BRR with a k_{BRR} of $5.0 (\pm 0.1) \times 10^{-4}$ cm s^{−1}.



Table 1 Transfer coefficients and rate constants for the BOR in 5.0 mM NaBr in 0.1 M HNO₃ and the BRR in 5.0 mM bromine in 0.1 M HNO₃ obtained at the glassy carbon macroelectrode GC, and single MWCNT impact current

Analysed parameter	Oxidation of bromide	Reduction of bromine
Transfer coefficient (GC)	$\beta = 0.45$	$\alpha = 0.33$
Transfer coefficient (impact current)	$\beta = 0.42$	$\alpha = 0.20$
$k_{\text{BOR}}/\text{cm s}^{-1}$ (GC)	$9.5 (\pm 0.1) \times 10^{-5}$	$2.0 (\pm 0.1) \times 10^{-5}$
$k_{\text{BRR}}/\text{cm s}^{-1}$ (impact current)	$1.0 (\pm 0.1) \times 10^{-3}$	$5.0 (\pm 0.1) \times 10^{-4}$

10^{-4} cm s⁻¹ respectively. The transfer coefficients and rate constants obtained from impacts were compared to the voltammograms obtained at pristine GC for the BOR and BRR and are given in Table 1. It is clearly evident that MWCNTs show some, albeit modestly, improved catalytic activity towards the Br₂/Br⁻ redox reaction when compared to the pristine GC electrode.

In summary, MWCNTs were studied for their catalytic behaviour towards the Br₂/Br⁻ redox couple. From the drop-cast experiment, the ensemble of MWCNTs showed mixed mass transport behaviour complicating and precluding the elucidation of their catalytic behaviour. In contrast, single nano-impact electrochemistry of MWCNTs shows faster electrochemical rate constants compared to pristine GC. This confirms the catalytic activity of MWCNTs for the Br₂/Br⁻ redox reaction but the values determined are insufficiently enhanced over glassy carbon leaving considerable room for improvement *via* the use of alternative electrocatalysts to carbon nanotubes.

Author contributions

A. K. S – performed experiments, investigation, formal analysis, data curation, and writing – original draft. R. M – writing – review and editing. D. L – writing – review and editing. RGC – conceptualisation, resources, supervision, and writing – review and editing.

Conflicts of interest

The authors declare no conflict of interest.

Acknowledgements

A. K. S. thanks the Commonwealth Scholarship Commissions, UK and University of Oxford for funding her DPhil research. We thank Prof Angela J. Russel and Dr Carole Bataille for helping us by providing a sample of bromine.

References

- 1 M. C. Wu, T. S. Zhao, H. R. Jiang, Y. K. Zeng and Y. X. Ren, *J. Power Sources*, 2017, **355**, 62–68.
- 2 G. Lin, P. Y. Chong, V. Yarlagadda, T. V. Nguyen, R. J. Wycisk, P. N. Pintauro, M. Bates, S. Mukerjee, M. C. Tucker and A. Z. Weber, *J. Electrochem. Soc.*, 2016, **163**, A5049–A5056.
- 3 Q. Chen, L. Eisenach and M. J. Aziz, *J. Electrochem. Soc.*, 2016, **163**, A5057–A5063.
- 4 M. Skyllas-Kazacos, G. Kazacos, G. Poon and H. Verseema, *Int. J. Energy Res.*, 2010, **34**, 182–189.
- 5 D. P. Scamman, G. W. Reade and E. P. L. Roberts, *J. Power Sources*, 2009, **189**, 1220–1230.
- 6 C. Wang, X. Li, X. Xi, W. Zhou, Q. Lai and H. Zhang, *Nano Energy*, 2016, **21**, 217–227.
- 7 H. T. Chen, A. K. S. Kumar, H. N. Le and R. G. Compton, *J. Electroanal. Chem.*, 2020, **876**, 114730.
- 8 W. I. Jang, J. W. Lee, Y. M. Baek and O. O. Park, *Macromol. Res.*, 2016, **24**, 276–281.
- 9 X. Rui, A. Parasuraman, W. Liu, D. H. Sim, H. H. Hng, Q. Yan, T. M. Lim and M. Skyllas-Kazacos, *Carbon*, 2013, **64**, 464–471.
- 10 Y. B. Yan, J. W. Miao, Z. H. Yang, F. X. Xiao, H. B. Yang, B. Liu and Y. H. Yang, *Chem. Soc. Rev.*, 2015, **44**, 3295–3346.
- 11 Q. Cao, Z. Shao, D. K. Hensley, N. V. Lavrik and B. J. Venton, *Langmuir*, 2021, **37**, 2667–2676.
- 12 I. Streeter, G. G. Wildgoose, L. D. Shao and R. G. Compton, *Sens. Actuators, B*, 2008, **133**, 462–466.
- 13 M. J. Sims, N. V. Rees, E. J. F. Dickinson and R. G. Compton, *Sens. Actuators, B*, 2010, **144**, 153–158.
- 14 G. P. Keeley and M. E. G. Lyons, *Int. J. Electrochem. Sci.*, 2009, **4**, 794–809.
- 15 E. Katelhon and R. G. Compton, *Appl. Mater. Today*, 2020, **18**, 100514.
- 16 L. F. Chen, E. Katelhon and R. G. Compton, *Appl. Mater. Today*, 2020, **18**, 100480.
- 17 S. V. Sokolov, S. Eloul, E. Kätelhon, C. Batchelor-McAuley and R. G. Compton, *Phys. Chem. Chem. Phys.*, 2017, **19**, 28–43.
- 18 W. Cheng and R. G. Compton, *TrAC, Trends Anal. Chem.*, 2014, **58**, 79–89.
- 19 X. T. Li, C. Batchelor-McAuley, L. D. Shao, S. V. Sokolov, N. P. Young and R. G. Compton, *J. Phys. Chem. Lett.*, 2017, **8**, 507–511.
- 20 K. J. Stevenson and K. Tschulik, *Curr. Opin. Electrochem.*, 2017, **6**, 38–45.
- 21 X. Li, C. Batchelor-McAuley, S. A. I. Whitby, K. Tschulik, L. Shao and R. G. Compton, *Angew. Chem.*, 2016, **55**, 4296–4299.
- 22 X. T. Li, H. Hodson, C. Batchelor-McAuley, L. D. Shao and R. G. Compton, *ACS Catal.*, 2016, **6**, 7118–7124.
- 23 X. T. Li, C. Batchelor-McAuley, K. Tschulik, L. D. Shao and R. G. Compton, *Chemphyschem*, 2015, **16**, 2322–2325.
- 24 R. E. White and S. E. Lorimer, *J. Electrochem. Soc.*, 1983, **130**, 1096–1103.
- 25 X. T. Li, C. Batchelor-McAuley, S. A. I. Whitby, K. Tschulik, L. D. Shao and R. G. Compton, *Angew. Chem., Int. Ed.*, 2016, **55**, 4296–4299.
- 26 A. Krittayavathananon, K. Ngamchuea, X. T. Li, C. Batchelor-McAuley, E. Katelhon, K. Chaisiwamongkhon, M. Sawangphruk and R. G. Compton, *J. Phys. Chem. Lett.*, 2017, **8**, 3908–3911.

